

# Crack Initiation and Growth Behaviour of Smooth Specimens Cut from the Squeeze Cast Al Alloy Car Wheels

M. Goto<sup>1</sup>, T. Yamamoto<sup>1</sup>, H. Nisitani<sup>2</sup> and N. Kawagoishi<sup>3</sup>

<sup>1</sup> Dept. of Mechanical Engineering, Oita University, Oita, 870-1192, Japan

<sup>2</sup> Dept. of Mechanical of Engng, Kyusyu-Sangyo University, Fukuoka, Japan

<sup>3</sup> Dept. of Mechanical Engng, Kagoshima University, Kagoshima, Japan

***ABSTRACT:** In order to clarify the crack initiation and propagation behaviour of a squeeze cast aluminum-silicon-magnesium alloy, fatigue tests of smooth specimens cut from Al alloy car wheels formed by the squeeze casting were carried out under the constant stress amplitudes. The behaviour of microcracks was monitored successively by the plastic replication method. In addition to the constant stress amplitude tests, fatigue tests under the two-step loading (low-to-high block and high-to-low block loading) were performed. The physical basis of the effect of stress change on fatigue damage was investigated based on the behaviour of small cracks.*

## INTRODUCTION

Since the aluminum casting alloys have been superior in light weight, high productivity, cost performance, recyclability, etc., those alloys have been widely used for the machine and structure. On the other hand, a serious problem for use of casting alloys to the components is a low fatigue strength and a low reliability caused from the casting defects like shrinkage cavities peculiar to the casting alloys [1]. The squeeze casting has dramatically improved the mechanical properties, fatigue characteristics and reliability of strengths of aluminum casting alloy [2-4]. The improvements result from the fine microstructure and the suppression of micro defects such as pinhole, shrinkage porosity. Recently, many fatigue data of squeeze cast Al alloy have been reported. Most of those data were gathered from the materials cast for the specimen use. However, there are few data obtained from the material cut from the actual machine components.

In the present study, fatigue tests of smooth specimens cut from squeeze cast Al alloy car wheels were carried out to clarify the crack initiation and propagation behavior under the constant stress amplitude. The behaviour of microcracks was monitored successively by the plastic replication method. To minimize the scatter in fatigue data due to the fluctuation of laboratory atmosphere, the machine was placed in a small cabin in the laboratory. The

temperature and humidity in the cabin were kept under control ( $t = 30^{\circ}\text{C}$ ,  $h = 60\%$ ). All the tests were made in controlled air. In addition to this, fatigue tests under the two-step loading in the controlled air were performed to study the effect of stress change on the behaviour of a small crack.

## EXPERIMENTAL PROCEDURES

The material was an aluminum-silicon-magnesium casting alloy (JIS: AC4CH). The material was cut from the car wheels formed by a vertical squeeze-casting machine. After the casting, all the wheels were solution treated, followed by ageing. The mechanical properties after the heat treatment were 214 MPa 0.2% proof stress, 263 MPa ultimate tensile strength, 337 MPa true breaking stress, and 27.3% reduction of area.

The round bar specimens with 5mm diameter were machined from the bars cut from the disk portion (thickness: 15mm) of the car wheels. Although the specimens have a shallow circumferential notch (depth:  $t = 0.25\text{mm}$ , radius:  $\rho = 20\text{mm}$ ), the strength reduction factor for this geometry is close to unity, so that the specimens can be considered as plain specimens. Before testing, all the specimens were electropolished to remove about  $20\mu\text{m}$  from the surface layer, in order to facilitate the observations of changes in the surface state.

All the tests were carried out using a rotating bending fatigue machine with a capacity of 100 Nm operating at 50 Hz. The specimens were fatigued at room temperature in air under the constant stress amplitude and the two-step loading (low-to-high and high-to-low block loading). To minimize the effect of fluctuation of atmosphere on the fatigue tests, the machine was placed in a small cabin in the laboratory. The temperature and humidity in the cabin were kept under control;  $t = 30^{\circ}\text{C}$ ,  $h = 60\%$ .

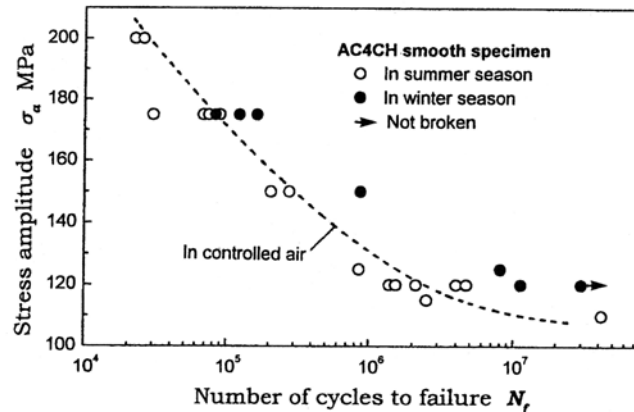
The observation of fatigue damage on the surface and the measurements of crack length were made via plastic replicas using an optical microscope at a magnification of  $\times 400$ . The value of stress,  $\sigma_a$ , means the nominal stress amplitude at the minimum cross section.

## EXPERIMENTAL RESULTS AND DISCUSSION

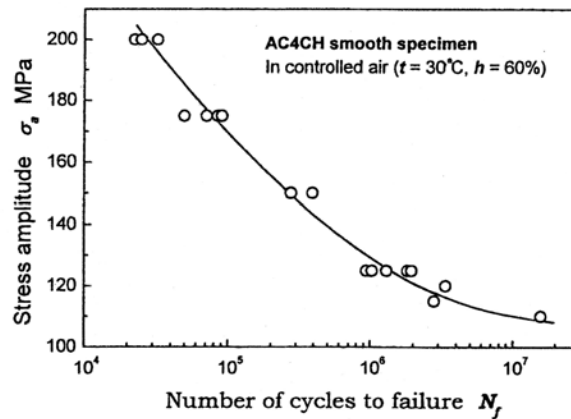
### *Fatigue damage under the constant stress amplitude*

Figure 1 shows the S-N curve in uncontrolled laboratory air. The  $\circ$  and  $\bullet$  symbols show the experimental data gathered in summer- and winter-season, respectively. The influence of atmosphere on fatigue strength is clearly recognized. Fig.2 shows the S-N curve in controlled laboratory air ( $t$

= 30°C,  $h = 60\%$ ). Scatter in the fatigue strength is dramatically decreased when compared to the uncontrolled air (Fig.1). The fatigue limiting stress at  $10^7$  cycles is  $\sigma_w = 110\text{MPa}$  in the controlled atmosphere. To minimize the scatter in the fatigue data due to the fluctuation of laboratory atmosphere, all the tests were carried out in controlled laboratory air.



**Figure 1:** S-N curve in uncontrolled laboratory air.



**Figure 2:** S-N curve in controlled laboratory air.

Figure 3 shows the S-N curves and 0.03mm crack initiation curves normalized by the ultimate tensile strength,  $\sigma_U$ . The relations for an age hardened Al alloy 6061-T6 (Al-Si-Mg alloy) are compared to the present material, AC4CH. The tensile strength of 6061-T6 was  $\sigma_U = 309\text{MPa}$  which is larger than AC4CH ( $\sigma_U = 263\text{MPa}$ ). There are negligible differences in

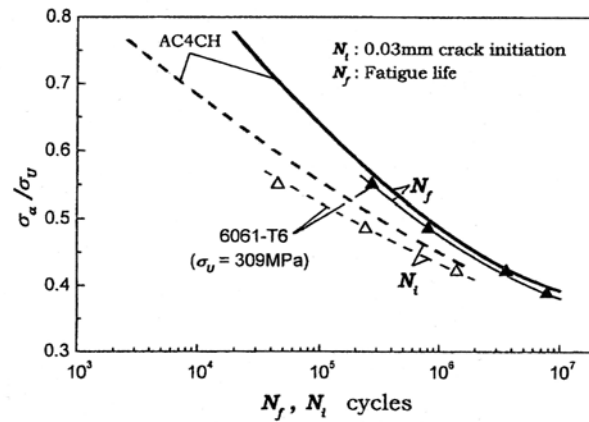


**Figure 3:**  $\sigma_a/\sigma_U$  versus  $N_f$  and  $N_i$ , 0.03mm crack initiation life, relation.

S-N curves. Thus, it can be concluded that the fatigue strength of squeeze cast Al alloy cut from the car wheel is comparable to 6061-T6 alloy. This may relate to that the specimens were cut from thick portion in the wheels where include few defects. Accordingly, the present data never represent the fatigue strength for actual car wheel, however it may be convenient for the consideration of the average fatigue characteristics of the material used for the car wheels. On the other hand, 0.03mm crack initiation life at the same  $\sigma_a/\sigma_U$  is longer in AC4CH than 6061-T6.

The initiation and growth behaviour of cracks was monitored by the plastic replication technique. Results showed that, at an early stage of cycling, cracks were initiated at or near the interfaces between the matrix and eutectic Si particles. Some cracks were initiated from a slip band in the matrix, however no cracks initiated from the defects such as pinholes and shrinkage porosities were observed. After the initiation, the growth behaviour of a small crack was influenced by the microstructure.

Figure 4 shows the  $\ln l$  vs.  $N/N_f$  relation for  $\sigma_a = 125\text{MPa}$ . Large scatter in the relation is recognized when the stress is relatively low. However, the scatter tended to decrease with an increase in stress amplitude. Fig. 5 shows the comparison of the  $\ln l$  vs.  $N/N_f$  relation under various stress amplitudes. The relation depends on the stress amplitude.

Figure 6 shows the  $dl/dN$  vs.  $l$  relation. For all the stress amplitudes, the change in the relation occurs at around  $l = 0.3\text{mm}$ . Namely, the relation for  $l > 0.3\text{mm}$  can be approximated by the straight line. Its slope is about unity when  $\sigma_a \geq 150\text{MPa}$ . On the other hand, the relation for  $l < 0.3\text{mm}$  is accelerated from the extension of the relation for a large crack ( $l > 0.3\text{mm}$ ). This acceleration comes from the difference in the crack growth mode, i.e., dominant growth mode tends to change from shear to tensile at  $l \approx 0.3\text{mm}$ .

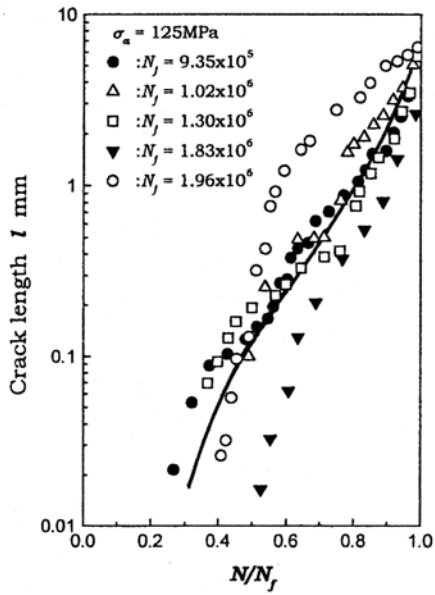


Figure 4:  $\ln l$  vs.  $N/N_f$  relation for  $\sigma_a = 125$  MPa.

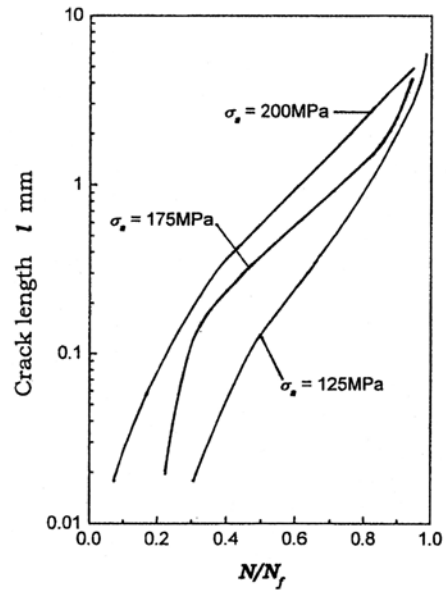


Figure 5: Comparison of the  $\ln l$  vs.  $N/N_f$  relation for various stresses.

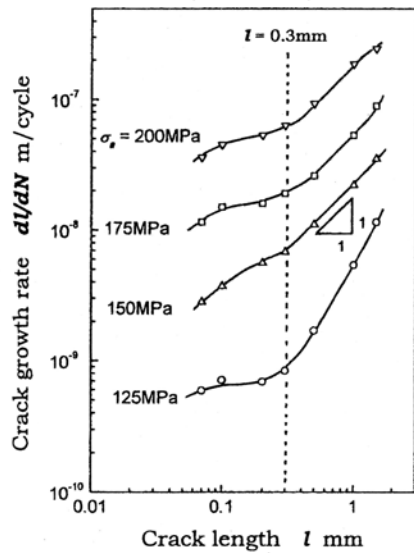


Figure 6:  $dl/dN$  vs.  $l$  relation.

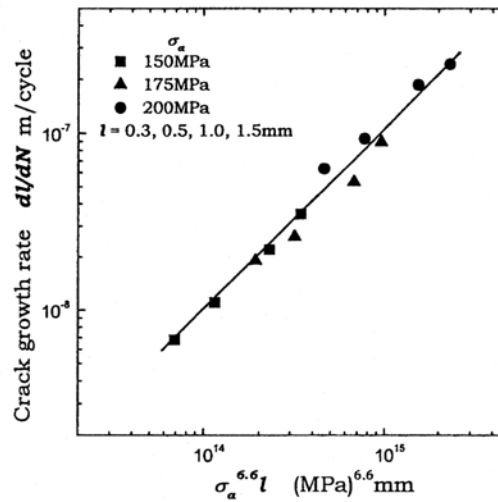


Figure 7:  $dl/dN$  vs.  $\sigma_a^n l$  relation.

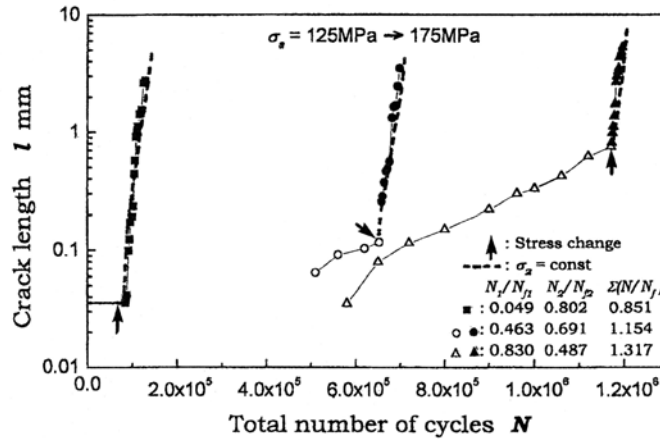
Figure 7 shows the  $dl/dN$  vs.  $\sigma_a^n l$  relation ( $n = 6.6$ ) [5]. The growth rate of a crack larger than 0.3mm under a large stress ( $\sigma_a \geq 150$ MPa) is

determined by a small crack growth law.

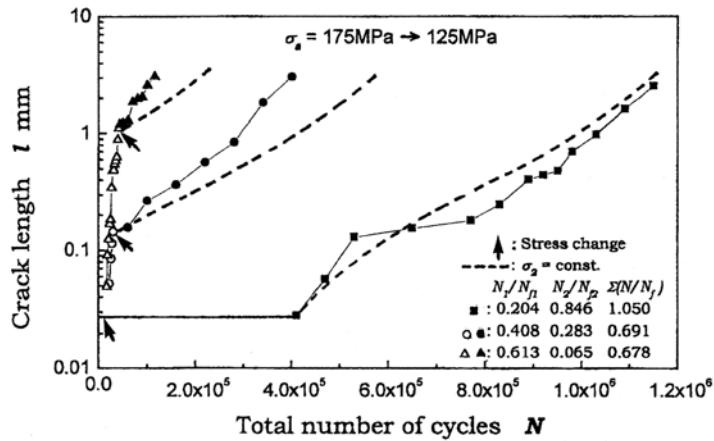
**Fatigue damage under the two-step loading**

The stresses used for the two-step loading were  $\sigma_a = 125$  and  $175$  MPa. The mean fatigue life under the constant stress amplitude was  $N_f = 1.409 \times 10^6$  cycles (average of 5 specimens) for  $\sigma_a = 125$  MPa and  $N_f = 7.42 \times 10^4$  cycles (average of 4 specimens) for  $\sigma_a = 175$  MPa.

Figure 8 shows the crack growth curve for (a) low-to-high and (b) high-to-low block loading. The  $\uparrow$  symbol indicate the position where the



(a) Low-to-high block loading.

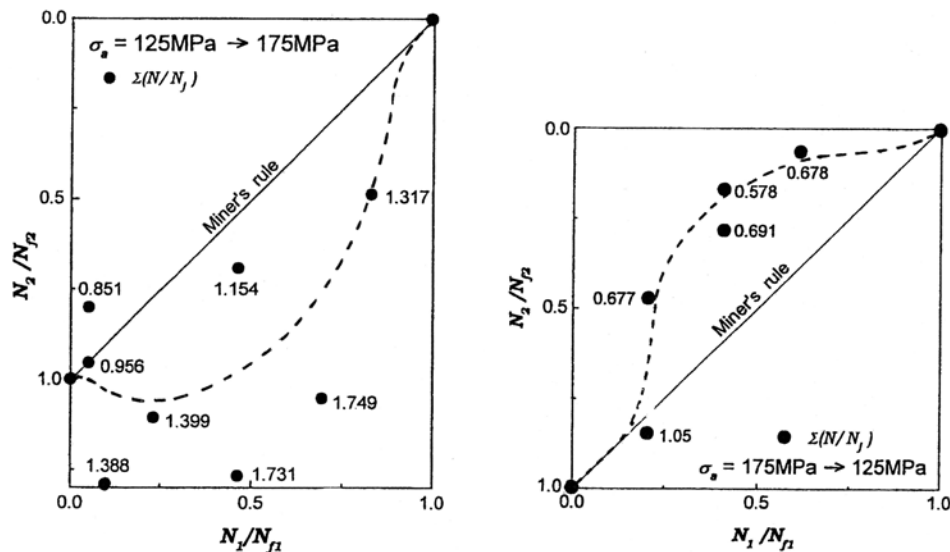


(b) High-to-low block loading.

**Figure 8:** Crack growth curve under two-step loading.

stress is changed from  $\sigma_1$  to  $\sigma_2$ ,  $\sigma_1$  and  $\sigma_2$  being the first and second stress levels, respectively. The dashed lines show the growth curve under the constant stress of  $\sigma_2$  (no repetitions of  $\sigma_1$ ). For the case of low-to-high block loading, there is no significant difference between the growth data after the stress change and each dashed line. Thus, the crack growth behaviour under  $\sigma_2$  is not affected by the history of the first stress cycling. On the other hand, for the case of high-to-low block loading, the growth rate under the second stress is accelerated when compared to the dashed lines which represent crack growth curves under the constant stress of  $\sigma_2$ . However, when the stress is changed before crack initiation (■ symbol), no effect of the first stress on the growth behaviour under  $\sigma_2$  is observed. Although the mechanism for the acceleration of crack growth is not clear, it may result from decreased crack closure and cyclic softening at the heavily deformed region around a crack tip caused by the loading under  $\sigma_1$ . Such a decreased crack closure may result from the large opening ratio of a crack generated at a high stress  $\sigma_1$ .

Figure 9 shows the values of cumulative cycle ratio; (a) low-to-high and (b) high-to low block loading. All the values of  $\Sigma(N/N_f)$  are within the range  $0.578 < \Sigma(N/N_f) < 1.749$ . For low-to-high block loading, the values of  $\Sigma(N/N_f)$  are larger than unity. The values of  $\Sigma(N/N_f) > 1$  can be explained from no effect of the history of the first stress cycling on the subsequent



(a) Low-to-high block loading. (b) High-to-low block loading.

**Figure 9:** Values of cumulative cycle ratio under the two-step loading.

growth behaviour under  $\sigma_2$  and the stress dependency of the  $\ln l$  vs  $N/N_f$  relation (Fig.5). For high-to-low block loading, however, the values of  $\Sigma(N/N_f)$  is smaller than unity. The values of  $\Sigma(N/N_f) < 1$  results from the acceleration of crack growth after the stress change and the stress dependency. Thus, when examining the fatigue damage under complex loading, it should be taken into account that  $\Sigma(N/N_f)$  has a distinct tendency determined by the loading pattern and stress levels used for the tests.

## CONCLUSIONS

Fatigue tests of smooth specimens of AC4CH (Al-Si-Mg alloy) cut from squeeze cast car wheels were carried out to clarify the crack initiation and growth behavior under the constant stress amplitude and two-step loading.

The main conclusions may be summarized as follows:

1. The fatigue strength based on the tensile strength is comparable to the 6061-T6 (Al-Si-Mg alloy). This may relate to that the specimens were cut from the thick portion of the wheels where includes few defects.
2. Fatigue cracks were initiated principally from the interfaces between the matrix and eutectic Si particles, and sometimes from a slip band in the matrix. But, no initiation from the microscopic defects was observed.
3. The  $\ln l$  vs.  $N/N_f$  relation under the constant stress exhibited stress dependency (the crack length at the same  $N/N_f$  is larger in higher stress).
4. For a crack less than 0.3mm, shear mode growth was predominantly observed and the microstructure strongly affected growth behaviour. When the stress is relatively high ( $\sigma_a \geq 150\text{MPa}$ ),  $dl/dN$  of a crack larger than 0.3mm was determined uniquely by a term  $\sigma_a^n l$  ( $n = 6.6$ ).
5. With regard to the fatigue damage under the two-step loading, the cumulative cycle ratio  $\Sigma(N/N_f)$  for the low to high block loading was smaller than unity, however it was larger than unity for the high to low block loading. The value of  $\Sigma(N/N_f)$  was closely related to the growth characteristics of a small crack.

## REFERTENCES

1. Bailey, W.A. (1965) *Foundry* **93**, 96.
2. Kaneko, Y., Murakami, H., Kuroda, K. and Nakazaki, S. (1980) *Foundry Trade Journal* **28**, 397.
3. Williams, G. (1984) *Foundry Trade Journal* **2**, 66.
4. Inguanty, P.C. (1985) *Proc. 17th National SAMPE Technical Conference*, 61.
5. Nistani, H. and Goto, M. (1986) *The Behaviour of Short Fatigue Cracks* (Ed. Miller, K.J. and los Rios, E.R.) EGF-1, 461.